

## EFFECT OF THE CONCENTRATION OF SILVER NANOPARTICLES ON THE PHOTOCATALYTIC ACTIVITY OF TITANIUM DIOXIDE NANORODS

Kayumova A.S., Serikov T.M. \*, Omarova G.S., Dzhakupova M.S.

Karaganda Buketov University, Karaganda, Kazakhstan, serikov-timur@mail.ru

*In this paper the results of a study of the effect of the concentration of silver nanoparticles in films of titanium dioxide nanorods on their photocatalytic activity are presented. Titanium dioxide nanorods with a rutile structure was obtained using the method of hydrothermal synthesis. Due to changing with the amount of substance of the transition metal silver salt ( $\text{AgNO}_3$ ) and chemical reduction on the surface of the titanium dioxide nanorods, Ag nanoparticles of different concentrations were obtained. The photocatalytic activity of the samples was assessed by the amount of photocurrent obtained from a unit of film surface and photodegradation of methylene blue dye when illuminating the surface with a light source of a Xenon lamp. Surface morphologies and energy dispersive X-ray studies showed that Ag nanoparticles were uniformly distributed and anchored on the titanium dioxide nanorods surface.*

**Keywords:** nanorods, titanium dioxide, silver nanoparticles, Ag, photocatalysis

### 1. Introduction

Titanium dioxide  $\text{TiO}_2$  is one of the most researched and widely used materials for water purification, air purification, hydrogen production and solar cells due to its many advantages and unique physical and chemical properties [1-4]:

1. Low cost:  $\text{TiO}_2$  is cheap and readily available, making it attractive for mass production.
2. Chemical stability:  $\text{TiO}_2$  is chemically stable and does not degrade in aggressive environments, which allows it to be used in various conditions.
3. Suitable zone position:  $\text{TiO}_2$  zones are suitable for inducing oxidation and reduction reactions, making it effective for a variety of catalyst processes.
4. Non-toxic and biocompatible:  $\text{TiO}_2$  is a non-toxic and biocompatible material, which is important for medical and biological applications.
5. Possibility of controlling the geometric structure, depending on the synthesis method, for example nanorods, nanotubes, nanofilaments and  $\text{TiO}_2$  nanoparticles [5-9].

However, despite the many structures,  $\text{TiO}_2$  has two main disadvantages: firstly, it can only absorb ultraviolet radiation due to its wide band gap (~3.2 eV), secondly, its high photogenerated carrier recombination rate leads to low quantum efficiency [10, 11].

Among the variety of nanostructures, titanium dioxide nanorods (TNR) are the most promising because they have one-dimensional electron transport, high specific surface area and high crystallinity [12-14]. At the same time, the possibility of using one-dimensional electron transport will make it possible to somehow reduce the recombination rate of photogenerated TNR charge carriers, but the problem of the absorption capacity of only the ultraviolet region has not yet been resolved.

The spectral sensitivity of TNR in the visible range can be expanded by adding noble metal nanoparticles [15, 16], sensitization with dye molecules [17], and adding nanomaterials with lower band gap energy [18-20]. The introduction of Ag nanoparticles into the  $\text{TiO}_2$  structure is an effective method for improving its photocatalytic properties. The introduction of Ag nanoparticles into  $\text{TiO}_2$  is an effective method for improving its photocatalytic properties. On the one hand, a Schottky barrier can form between  $\text{TiO}_2$  and Ag nanoparticles [21, 22], restraining the reverse current of injected electrons from  $\text{TiO}_2$  to Ag and thereby suppressing the recombination of electron-hole pairs. On the other hand, Ag nanoparticles generate localized surface plasmon resonance (LSPR) effect under visible light, and excited hot electrons can be

injected onto the TiO<sub>2</sub> surface [23, 24]. Thus, the performance of TiO<sub>2</sub>/Ag composite is superior to that of TiO<sub>2</sub> [25]. Despite the huge number of published works on the photocatalytic activity of TNR and the use of LSPR in these processes, there is no information on the optimal concentration of Ag nanoparticles on the surface of TiO<sub>2</sub> nanorods obtained by chemical method.

The purpose of this work is to determine the optimal concentration of Ag nanoparticles on the surface of TNR films at which the best photocatalytic activity will be observed.

## 2. Experimental part

TNRs are synthesized by hydrothermal synthesis. Cleaned fluorine-doped tin oxide (FTO) substrates were prepared from a solution containing 7.5 ml - of deionized water, 7.5 ml of hydrochloric acid, and 0.25 ml of titanium butoxide C<sub>16</sub>H<sub>36</sub>O<sub>4</sub>Ti - in a 25 ml fluoroplastic embedded stainless steel tube was placed in an autoclave. The solution was kept in a furnace for 6 hours at a temperature of 180°C. The samples were then removed and washed with deionized water. To improve crystallization and remove synthesis byproducts, the nanorods films were heated in a high temperature oven at 500°C for 2 hours.

Ag nanoparticles were prepared by chemical deposition method. 0.2 g of polyvinylpyrrolidone was added to 40 ml of H<sub>2</sub>O and C<sub>2</sub>H<sub>6</sub>O<sub>2</sub> (1:1% by volume), then 2 mmol of NaBH<sub>4</sub> was added to the solution mixture with vigorous stirring. The resulting mixture was stirred for about 5 minutes. Then 0.5, 0.75, 1 and 2 mmol AgNO<sub>3</sub> were added at different concentrations. Substrates containing TNR were dipped upwards into the bottom of the dish and kept in an oven at 70°C for 2 minutes. The sample was then washed with deionized water and dried at room temperature.

Using a scanning electron microscope Mira 3MLU from Tescan at a voltage of 20 kV, a study of surface morphology, energy dispersive X-ray analysis (EDX) analysis and distribution of elements on the surface was carried out. Spectrophotometric measurements were carried out on a Solar CM 2203 scanning spectrophotometer (Solar) in the wavelength range 190-750 nm.

The resistance of the films was determined using impedance spectroscopy. For this purpose, the working electrode (test samples) and the counter electrode made of Pt (Platisol T/SP, Solaronix) deposited on FTO were glued together with a polymer film 25 μm thick (Melotonix, Solaronix). Iodide/triiodide electrolyte (Iodolyte Z-150, Solaronix) was used as the electrolyte.

The photocatalytic activity of the samples was assessed by measuring the photoinduced current with an illuminated area of 1 cm<sup>2</sup> in a standard three-electrode cell using a CS350 potentiostat/galvanostat with a built-in EIS analyzer (Corrtest Instruments, China). Platinum foil served as the counter electrode, and an AgCl electrode was used as the reference electrode. The measurements were carried out in a 0.1 mmol NaOH electrolyte in a specially manufactured photoelectrochemical cell with a quartz window. In addition, the photoactivity of the films was assessed by the photodegradation of the dye methylene blue (MB), which is used as a model pollutant. The radiation source used in the experiments was a xenon lamp with a power of 300 W/cm<sup>2</sup> (Newport, USA).

## 3. Results and discussion

Figure 1 shows micrographs of the surface morphology of the TNR film before and after deposition of Ag nanoparticles. From Figure 1a, it can be seen that hydrothermal synthesis produces titanium dioxide nanorods on the surface of the FTO substrate, predominantly perpendicular to the substrate surface. The length of the nanorods is about 1.48 μm, the average diameter of the nanorods is 50-60 nm. Chemical reduction of silver nitrate resulted in the formation of Ag nanoparticles on the surface of TNR (see Figure 1 b, c, d and f). The deposited Ag nanoparticles are uniformly distributed over the entire surface of the samples and envelop the walls of the TNR films, thereby creating roughness. It can be seen from the figures that with an increase in the concentration of AgNO<sub>3</sub> from 0.5 to 2 mmol used in reduction, the number of Ag nanoparticles increases.

This is especially noticeable from Figure 1d and 1f, where the concentration is 1 and 2 mmol. At the same time, the number of Ag nanoparticles is so large that the presence of TNR underneath is practically invisible. The sizes of silver nanoparticles were measured using the dynamic light scattering method on a Zetasizer Nano ZS. For this purpose, solutions were used from which Ag nanoparticles were deposited. It was found that the average diameter of nanoparticles is 25-30 nm, which is also confirmed by SEM image processing.

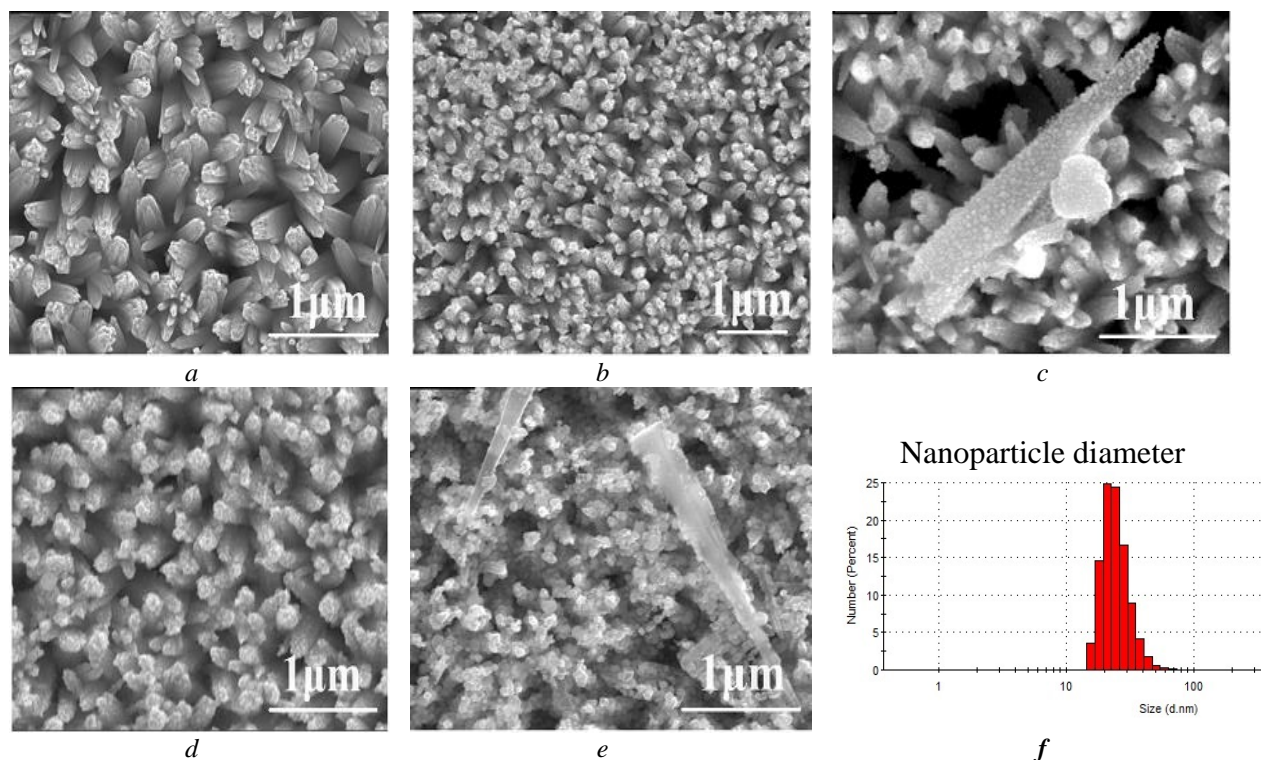


**Fig.1.** SEM images of the TNR surface before and after Ag deposition:

a) TNR; b) TNR/Ag\_0.5 mmol; c) TNR/Ag\_0.75 mmol; d) TNR/Ag\_1 mmol; e) TNR/Ag\_2 mmol; f) Diameter of nanoparticles measured on Zetasizer Nano

Surface mapping and EDX spectrum of TNR doped with Ag nanoparticles of different concentrations are presented in Figure 2. In all samples, 5 elements were identified, such as Ti, O, Ag, Na and Si. The elements Ti and O belong to the titanium dioxide nanorods that form the basis of the film, so its percentage is much higher than the others. The presence of peaks in the energy ranges from 3.4 to 4 keV and 1.8 keV, 1 keV correspond to the peaks of Sn, Si and Na, respectively, which belong to the FTO substrates. Peaks in the 3 keV region correspond to Ag nanoparticles.

Five spectra were taken from the surface of each sample: at the center and at the corners. The inset in Figure 2 shows the content of elements (in percentage) relative to the entire total spectrum of the map. From the data obtained, it is clear that with an increase in the amount of silver transition metal salt ( $\text{AgNO}_3$ ) used in chemical reduction, the concentration of reduced Ag nanoparticles on the TNR surface increases. Thus, with an amount of substance of 0.5 mmol  $\text{AgNO}_3$ , the proportion of Ag nanoparticles relative to the entire total spectrum was 2.3%, for 0.75, 1 and 2 mmol it was 2.8, 6.5 and 6.8%, respectively.

The normalized absorption spectra of the samples are presented in Figure 3. From the absorption spectra presented in Figure 3 it is clear that doping Ag NPs significantly expands the absorption spectrum of the photocatalyst relative to undoped  $\text{TiO}_2$ . The absorption peak of silver nanoparticles in the spectrum is located in the range of 410–420 nm. The introduction of Ag nanoparticles into TNR structures leads to an expansion of spectral sensitivity in the visible range.

This is confirmed by the pronounced small peaks of Ag nanoparticles in TNR/Ag nanocomposite materials in the region of 420–480 nm. In addition, TNR/Ag nanocomposites effectively absorb light in the ultraviolet region of the spectrum.

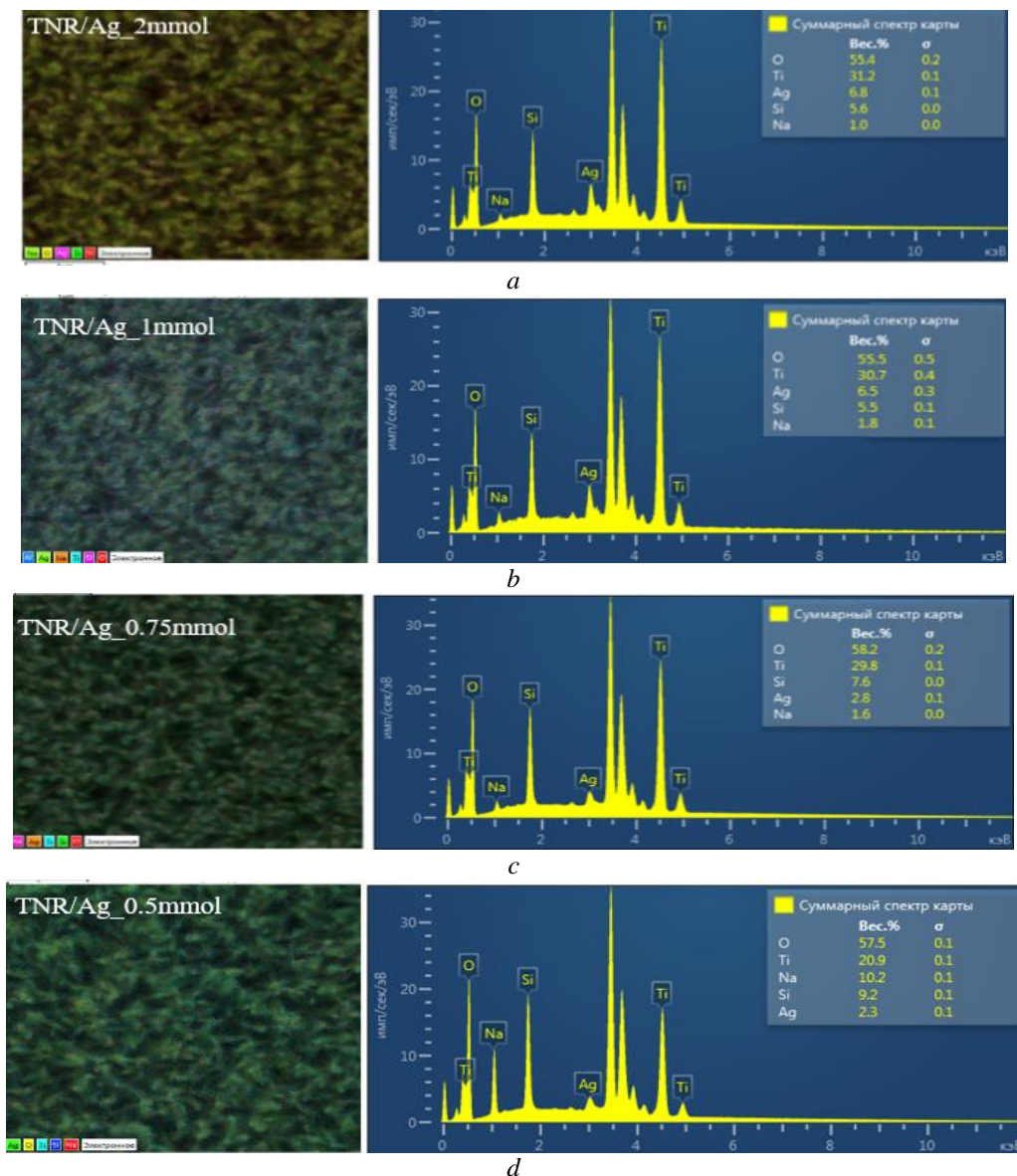


**Fig. 2.** Surface mapping and EDX spectrum of TNR doped with Ag nanoparticles of different concentrations: a) TNR/Ag\_2 mmol; b) TNR/Ag\_1 mmol; c) TNR/Ag\_0.75 mmol; d) TNR/Ag\_0.5 mmol.

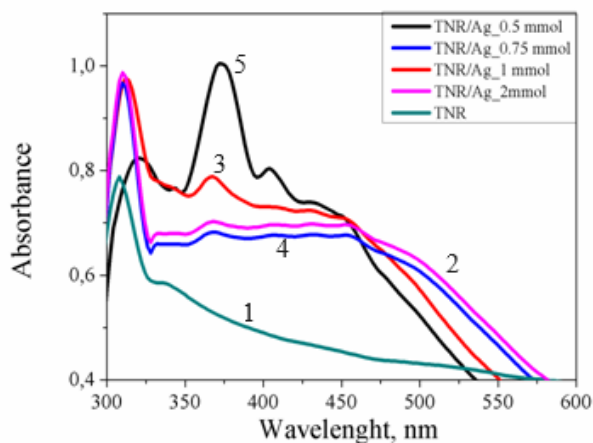
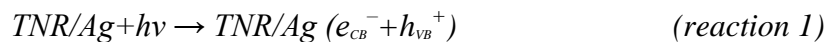


**Fig. 3.** Absorption spectrum of TNR/Ag at different concentrations: 1-TNR, 2- TNR/Ag\_2 mmol, 3-TNR/Ag\_1 mmol, 4-TNR/Ag\_0,75 mmol, 5-TNR/Ag\_0,5 mmol

The photocatalytic activity of the samples was assessed by the decomposition reaction of the dye methylene blue (MB) and it is a model pollutant. The process of photocatalytic oxidation is as follows: after irradiation and excitation of electrons from the valence band of the photocatalyst, photogenerated holes can directly oxidize the dye to a reactive intermediate (reaction 1) or lead to the formation of highly reactive oxidative hydroxyl radicals (OH•), leading to degradation and discoloration dye (reactions 2 and 3).



or



or



The initial concentration of the MB dye was  $10^{-6}$  mol/L. Before the experiment, the samples were kept in a different solution of the MB dye for 8 hours to eliminate errors associated with the adsorption of the dye on its surface. The original optical density of the MB dye was 0.55 at the wavelength of its 662 nm absorption maximum and was obtained per unit.

An example of the degradation process of the MV dye and its assessment by optical density are presented in Figure 4a. From this figure it can be seen that with an increase in the duration of radiation, the optical density of the dye decreases, which leads to its discoloration and degradation of molecules. Further, at the absorption peak of 662 nm, a change in the absorbance of the MB dye was observed in the presence of TNR and TNR/Ag films with different silver concentrations. The curves for changes in optical density or dye concentration in the absence and presence of nanocomposite films are presented in Figure 4b. From the presented data it is clear that during long-term irradiation of the dye without immersed films, its degradation is insignificant and amounts to only 7%. In the presence of the film formed by TNR, the degradation rate increased significantly and reached 40% in 180 minutes of radiation. In the presence of TNR films with condemned Ag nanoparticles, the rate of dye degradation increased. Thus, when using a TNR/Ag film with an amount of reduced silver nitrate of 0.5 mmol, the degradation was 48%, and for 0.75, 1 and 2 mmol it was 60, 81 and 70%, respectively (see Fig. 4b) for a similar irradiation time.

Also, the photocatalytic activity of the samples was assessed by the photocurrent response when irradiated with artificial sunlight with periodic switching on and off of the light. In the absence of illumination, the photocurrent of the samples is zero; when the light was turned on, the photocurrent density instantly increased for all samples. It can be seen from Figure 4c that the maximum photocurrent value under light illumination for the TNR/Ag\_1mmol sample is  $890 \mu\text{A}/\text{cm}^2$  and is the highest among all samples. It is clear from the data that with an increase in the amount of reduced  $\text{AgNO}_3$  and, accordingly, reduced Ag nanoparticles on the surface, TNR first increases the photocurrent density and then decreases, indicating the presence of an optimal concentration.

Figure 4d shows the impedance hodographs in the Nyquist coordinates for all the samples under study. According to the godograph M. Adachi, M. Sakamoto, J. Jiu, et al. according to the methodology proposed in his works, the main electrical transfer properties of films were calculated [26]. The electron transport resistance in the  $R_w$  nanocomposite and the  $R_k$  charge transport resistance will directly depend on the number of electrons coming from the number of free electrons. The charge transfer resistance  $R_k$  of TNR/Ag films at a concentration of 1 mmol is 2.5 times less than in a film with a concentration of 0.5 mmol and is 1748 Ohm and 685 Ohm. Effective electron lifetime  $\tau_{eff}$  in films and nanocomposite materials. According to the results obtained, the duration of the effective lifetime of an electron in a sample with a concentration of 1 mmol is also 2 times less than the other samples. As the silver concentration increases, the effective lifetime of an electron in the sample increases. Long electron lifetimes increase the probability of electron recombination. Ag on the surface of TNR can resist oxidizing agents from solution or, conversely, are oxidized, since silver is a strong oxidizing agent. Unlike other noble metals such as Pt or Au, when Ag nanoparticles are combined with TNR, the Fermi level of the metal is located near the conduction band of  $\text{TiO}_2$ , and a Schottky barrier cannot be formed.



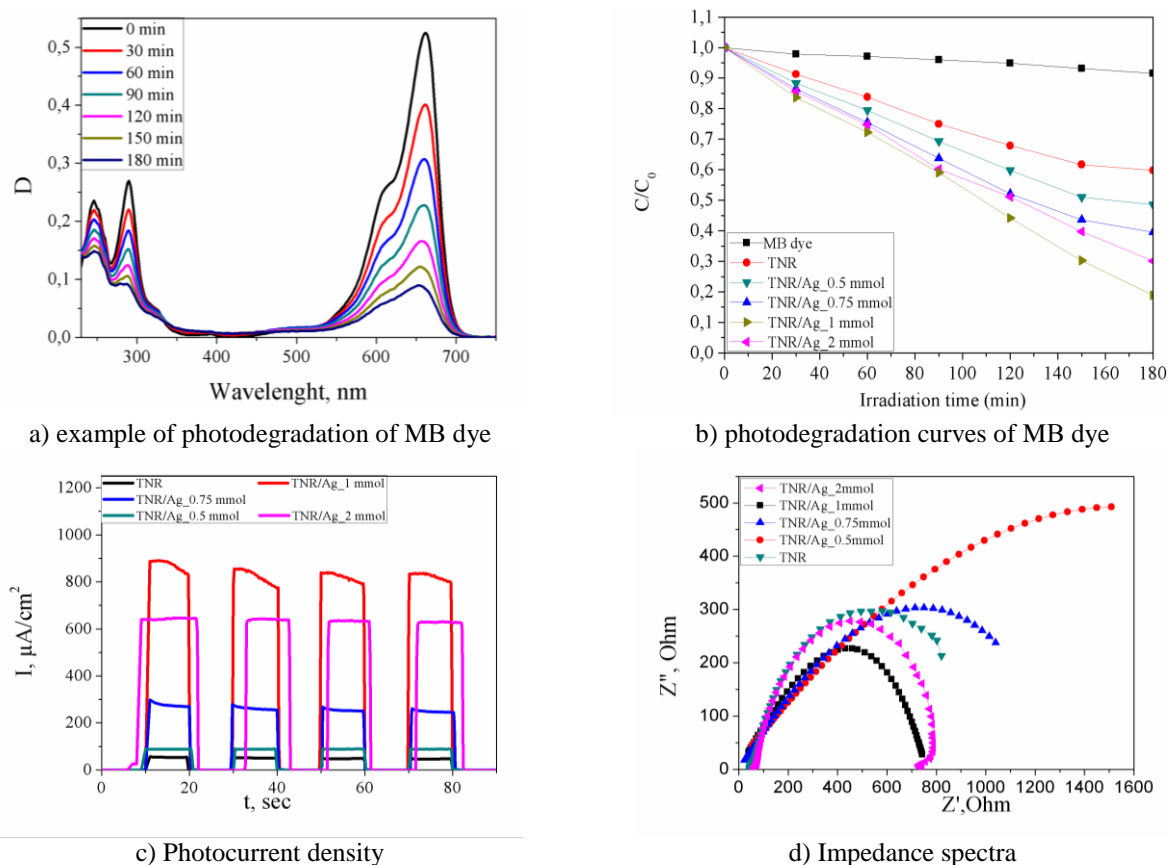


**Fig. 4.** Photocatalytic properties of TNR/Ag films at different concentrations.

Therefore, electrons can flow in both directions, allowing holes to be effectively captured by the silver particle. Researchers presented possible mechanisms of decomposition of various substances on the surface of  $\text{TiO}_2$  at different concentrations of silver nanoparticles [27]. However, they used  $\text{TiO}_2$  in nanoparticle form. The increase in photocatalytic activity of TNR in the presence of Ag may be due to the unusual electronic properties of silver and hot electrons, which are efficiently transferred to the conduction band of  $\text{TiO}_2$  and participate in photochemical reactions. The results obtained can be useful in creating effective photocatalysts for wastewater treatment and water splitting to produce hydrogen gas.

#### 4. Conclusions

Thus, the work compares  $\text{TiO}_2$  nanorods with a rutile structure, which were used to create composite materials with different concentrations of  $\text{AgNO}_3$ . From the results of the study, we can see that as the concentration of  $\text{AgNO}_3$  increases, its photocatalytic activity also increases. As the concentration of Ag nanoparticles on the TNR surface increases to 1 mmol, the photocatalytic activity increases and then decreases at 2 mmol, indicating the presence of an optimal concentration. The photocurrent density generated by a TNR film with a concentration of Ag nanoparticles of 1 mmol is 10 and 1.4 times higher than 0.5 mmol and 2 mmol, respectively. In the presence of a TNR film with a concentration of Ag nanoparticles of 1 mmol, the degradation of the dye reached 71%, which is 1.7 times higher than without Ag nanoparticles. The resistance of TNR/Ag films at a concentration of 1 mmol is 2.5 times less than that of a film with a concentration of 0.5 mmol.

#### REFERENCES

- 1 Ge M., Cao C., Huang J., et al. A review of one-dimensional  $\text{TiO}_2$  nanostructured materials for environmental and energy applications. *J. Mater. Chem. A*, 2016, Vol. 4., pp. 6772-6801. [doi: 10.1039/C5TA09323F](https://doi.org/10.1039/C5TA09323F)
- 2 Haider A.J., Jameel Z.N., Al-Hussaini I.M. Review on: titanium dioxide applications, *Energy Procedia*, 2019, Vol. 157, pp. 17-29. [doi: 10.1016/j.egypro.2018.11.159](https://doi.org/10.1016/j.egypro.2018.11.159)
- 3 Allahverdiyev A.M., Abamor E.S., Bagirova M., et al. Antimicrobial effects of  $\text{TiO}_2$  and  $\text{Ag}_2\text{O}$  nanoparticles against drug-resistant bacteria and leishmania parasites. *Future Microbiology*, 2011, Vol.6, pp. 933-940. [doi:10.2217/fmb.11.78](https://doi.org/10.2217/fmb.11.78)

- 4 Huang Z., Maness P.-C., Blake D. M. et al. Bactericidal mode of titanium dioxide photocatalysis. *Journal of Photochemistry and Photobiology A: Chemistry*, 2000, Vol.130, pp. 163–170. doi: [10.1016/s1010-6030\(99\)00205-1](https://doi.org/10.1016/s1010-6030(99)00205-1)
- 5 Serikov T.M., Ibrayev N. Kh., Savilov S.V., et al. T. M. Influence of the hydrothermal synthesis conditions on the photocatalytic activity of titanium dioxide nanorods. *Russian journal of applied chemistry*, 2021, Vol. 94, pp. 438–445. doi: [10.1134/S1070427221040030](https://doi.org/10.1134/S1070427221040030)
- 6 Serikov T.M., Ibrayev N. Kh., Isaykina O.Ya., et al. Nanocrystalline TiO<sub>2</sub> films: synthesis, low-temperature luminescent and photovoltaic properties. *Journal of Inorganic Chemistry*, 2021, Vol. 66, pp. 107–114. doi: [10.1134/S0036023621010071](https://doi.org/10.1134/S0036023621010071)
- 7 Fei Y.C., Ye X.F., Kang J.Y. Enhanced photocatalytic performance of TiO<sub>2</sub> nanowires by substituting noble metal particles with reduced graphene oxide. *Current applied physics*, 2022, Vol.44, pp.33–39. doi: [10.1016/j.cap.2022.09.008](https://doi.org/10.1016/j.cap.2022.09.008)
- 8 Mukametkalia T.M., Ilyassov B.R., Aimukhanov A.K., et al. Effect of the TiO<sub>2</sub> electron transport layer thickness on charge transfer processes in perovskite solar cells. *Physica B: Condensed Matter*, 2023, Vol. 659, pp. 414784. doi: [10.1016/j.physb.2023.414784](https://doi.org/10.1016/j.physb.2023.414784)
- 9 Serikov T.M., Baltabekov A.S., Aidarova D.D., et al. Effect of anodizing voltage on the photocatalytic activity of films formed by titanium dioxide nanotubes. *Eurasian Physical Technical Journal*, 2022, Vol.19, pp.28 – 33. doi: [10.31489/2022No4/28-33](https://doi.org/10.31489/2022No4/28-33)
- 10 Liu Y., Zhou Y., Yang L., et al. Hydrothermal synthesis of 3Durchin-like Ag/TiO<sub>2</sub>/reduced graphene oxide composites and its enhanced photocatalytic performance. *J Nanopart Res*, 2016, Vol.18, pp.283–295. doi: [10.1007/s11051-016-3596-6](https://doi.org/10.1007/s11051-016-3596-6)
- 11 Liang Y.T., Vijayan B.K., Gray K.A. et al. Minimizing graphene defects enhances titania nanocomposite-based photocatalytic reduction of CO<sub>2</sub> for improved solar fuel production. *Nano Lett*, 2011, Vol.11, pp.2865–2870. doi: [10.1021/nl2012906](https://doi.org/10.1021/nl2012906)
- 12 Cozzoli P.D., Kornowski A., Weller H. Low-temperature synthesis of soluble and processable organic-capped anatase TiO<sub>2</sub> nanorods, *Journal of the american chemical society*, 2003, Vol.47, pp.14539–14548. doi: [10.1021/ja036505h](https://doi.org/10.1021/ja036505h)
- 13 Xu J.M., Chen D.F., Wu J.F., et al. Nanowires-assembled TiO<sub>2</sub> nanorods anchored on multilayer graphene for high-performance anodes of lithium-ion batteries. *Nanomaterials*, 2022, Vol.12, pp.3697. doi: [10.3390/nano12203697](https://doi.org/10.3390/nano12203697)
- 14 Nada F. M., Saleem A.H., Shawki K.M. Hydrothermally growth of TiO<sub>2</sub> nanorods, characterization and annealing temperature effect. *Kuwait journal of science*, 2021, Vol.48, pp.3–6. doi: [10.48129/kjs.v48i3.10417](https://doi.org/10.48129/kjs.v48i3.10417)
- 15 Chakhtouna H., Benzeid H., Zari N. et al. Recent progress on Ag/TiO<sub>2</sub> photocatalysts: photocatalytic and bactericidal behaviors. *Environmental science and pollution research*, 2021, Vol.33, pp. 44638–44666. doi: [10.1007/s11356-021-14996-y](https://doi.org/10.1007/s11356-021-14996-y)
- 16 Gupta B., Melvin A.A., Matthews T., et al. TiO<sub>2</sub> modification by gold (Au) for photocatalytic hydrogen (H<sub>2</sub>) production. *Renewable & sustainable energy reviews*, 2016, Vol.58, pp. 1366–1375. doi: [10.1016/j.rser.2015.12.236](https://doi.org/10.1016/j.rser.2015.12.236)
- 17 Molinari R., Lavorato C., Argurio P. The Evolution of Photocatalytic Membrane Reactors over the Last 20 Years: A State of the rt Perspective. *Catalyst*, 2021, Vol.11, pp. 775. doi: [10.3390/catal11070775](https://doi.org/10.3390/catal11070775)
- 18 Stroyuk A.L., Kryukov A.I., Kuchmii S.Y. Semiconductor photocatalytic systems for the production of hydrogen by the action of visible light. *Theoretical and experimental chemistry*, 2009, Vol.45, No.4, pp.209–233. doi: [10.1007/s11237-009-9095-4](https://doi.org/10.1007/s11237-009-9095-4)
- 19 Karthikeyan C., Arunachalam P., Ramachandran K. Recent advances in semiconductor metal oxides with enhanced methods for solar photocatalytic applications. *Journal of alloys and compounds*, 2020, Vol.828, pp.154281. doi: [10.1016/j.jallcom.2020.154281](https://doi.org/10.1016/j.jallcom.2020.154281)
- 20 Dhinesh K.R., Thangappan R. R. Synthesis and characterization of LaFeO<sub>3</sub>/TiO<sub>2</sub> nanocomposites for visible light photocatalytic activity. *Journal of Physical and Chemistry of Solids*, 2016, Vol. 23, pp. PCS7876. doi: [10.1016/j.jpcc.2016.10.005](https://doi.org/10.1016/j.jpcc.2016.10.005)
- 21 Fu L., Zheng Y., Fu Z., et al. Synthesis of Ag decorated gra-phene-hierarchical TiO<sub>2</sub> nanocomposite with enhanced photocatalytic activity. *Funct Mater Lett*, 2015, Vol.8, pp. 1550036–1550039. doi: [10.1142/S1793604715500368](https://doi.org/10.1142/S1793604715500368)
- 22 Samir M., Geioushy R.A., El-Sherbiny S., et al. Enhancing the anti-ageing, antimicrobial activity and mechanical properties of surface-coated paper by Ag@TiO<sub>2</sub>-modified nanopigments, *Environmental science and pollution research*, 2022, Vol.29, pp. 72515–72527. doi: [10.1007/s11356-022-20935-2](https://doi.org/10.1007/s11356-022-20935-2)
- 23 Ke C.R., Guo J.S., Su Y.H., et al. The effect of silver nanopar-ticles/graphene-coupled TiO<sub>2</sub> beads photocatalyst on the photoconversion efficiency of photoelectrochemical hydrogen production. *Nanotechnology*, 2016, Vol.27, pp. 435405–435412. doi: [10.1088/0957-4484/27/43/435405](https://doi.org/10.1088/0957-4484/27/43/435405)
- 24 Paul K.K., Giri P.K. Role of Surface plasmons and hot electrons on the multi-step photocatalytic decay by defect enriched Ag@TiO<sub>2</sub> nanorods under visible light. *Journal of physical chemistry C*, 2017, Vol.36, pp.20016–20030. doi: [10.1021/acs.jpcc.7b05328](https://doi.org/10.1021/acs.jpcc.7b05328)
- 25 Serikov T.M., Kayumova A.S., Baltabekov A.S. et al. Photocatalytic activity of nanocomposites based on titania nanorods and nanotubes doped with Ag and reduced graphene oxide nanoparticles. *Nanobiotechnology Reports*, 2023, Vol. 18, pp. 207–215. doi: [10.1134/S2635167623700040](https://doi.org/10.1134/S2635167623700040)
- 26 Adachi M., Sakamoto M., Jiu J., et al. Determination of parameters of electron transport in dye-sensitized solar cells using electrochemical impedance spectroscopy. *J. Phys. Chem.B*, 2006, Vol. 110, pp. 13872. doi: [10.1021/jp061693u](https://doi.org/10.1021/jp061693u)
- 27 Wodka D., Bielańska E., Socha R.P., et al. Photocatalytic activity of titanium dioxide modified by silver nanoparticles. *ACS Applied Materials & Interfaces*, 2010, Vol. 2, pp.1945–1953. doi: [10.1021/am1002684](https://doi.org/10.1021/am1002684)